nature neuroscience

Corollary discharge circuits for saccadic modulation of the pigeon visual system

Yan Yang[1], Peng Cao[1,2], Yang Yang[1,2] & Shu-Rong Wang[1]

A saccadic eye movement causes a variety of transient perceptual sequelae that might be the results of corollary discharge. Here we describe the neural circuits for saccadic corollary discharge that modulates activity throughout the pigeon visual system. Saccades in pigeons caused inhibition that was mediated by corollary discharge followed by enhancement of firing activity in the telencephalic hyperpallium, visual thalamus and pretectal nucleus lentiformis mesencephali (nLM) with opposite responses in the accessory optic nucleus (nBOR). Inactivation of thalamic neurons eliminated saccadic responses in telencephalic neurons, and inactivation of both the nLM and the nBOR abolished saccadic responses in thalamic neurons. Saccade-related omnipause neurons in the brainstem raphe complex inhibited the nBOR and excited the nLM, whereas inactivation of raphe neurons eliminated saccadic responses in both optokinetic and thalamic neurons. It seems that saccadic responses in telencephalic neurons are generated by corollary discharge signals from brainstem neurons that are transmitted through optokinetic and thalamic neurons. These signals might have important roles in visual perception.

Humans and other foveate animals use rapid, darting eye movements (saccades) to search for or fixate a target of interest with the fovea. A variety of perceptual phenomena occur in temporal relation to the saccade. These include receptive field shifts that remap the visual field and maintain spatial constancy and begin in advance of the saccade[1–3], as well as compression of the perception of time and space[4,5]. Neural responses in relation to saccades have been found in the lateral geniculate nucleus (LGN)[6–8] and in cortical areas that receive magnocellular inputs in mammals[9–11]. Both the perceptual effects and at least some of the neural responses seem to be driven by corollary discharge related to the saccade, rather than by the rapid smearing of the visual scene during the saccade. Furthermore, corollary discharge through the thalamus contributes to the generation of spatially accurate saccades in monkeys[3,12]. Beyond this example, however, the neuronal circuits that underlie the changes in firing activity of visual neurons around a saccade are unclear.

Our understanding of the avian visual system offers a good opportunity to reveal neural circuits that mediate corollary discharge from the saccadic system. The telencephalic hyperpallium (Wulst) in birds receives input from the nucleus opticus principalis thalami (nOPT) (also called the LGN). In turn, nOPT receives afferents from the nLM and the nBOR of the accessory optic system[13,14]. These visual structures might be homologous to the striate cortex, LGN, the nucleus of the optic tract, and the terminal nuclei of the accessory optic tract in mammals, respectively (**Fig. 1**)[15,16]. Both the nBOR and the nLM, and their mammalian homologs, are involved in generating optokinetic nystagmus (OKN), which consists of slow and quick phases for stabilizing images on the retina[17–19]. Furthermore, the nBOR receives afferents from the raphe complex in the brainstem reticular formation[20], which in turn receives input from the optic tectum[21,22]. The tectum or superior colliculus[23–25] and reticular formation[25–27] are involved in saccadic eye movements in all the species of vertebrates that have been examined. Therefore, the optokinetic nuclei and brainstem reticular formation seem to be suitable candidates for modulating perisaccadic activity in telencephalic neurons using the nOPT as a relay station.

To provide physiological and anatomical evidence that the saccadic responses of telencephalic cells are modulated by corollary discharges from the optokinetic nuclei and the raphe complex through the nOPT, we used extracellular recording, activation and inactivation techniques in three steps. First, we recorded the responses of neurons in the telencephalon, nOPT, nLM, nBOR and raphe complex to saccades, to compare their firing patterns and time courses. Second, we used orthodromic and antidromic activation to reveal functional connections between optokinetic and raphe neurons. Third, we investigated the effects of thalamic blockade on telencephalic responses, the effects of nBOR and nLM blockade on thalamic responses and the effects of raphe inactivation on optokinetic and thalamic responses to saccades. These investigations provided consistent evidence that the optokinetic nuclei and raphe complex mediate the saccadic responses of telencephalic neurons via corollary discharge signals that pass through the thalamus.

RESULTS

We investigated the responses of 302 neurons (**Supplementary Table 1** online) during saccades and other interventions, consistently showing that the saccadic responses of telencephalic cells are driven by

[1]Laboratory for Visual Information Processing, State Key Laboratory of Brain and Cognitive Sciences, Institute of Biophysics, Chinese Academy of Sciences, 15 Datun Road, Beijing 100101, China. [2]These authors contributed equally to this work. Correspondence should be addressed to S.-R.W. (wangsr@sun5.ibp.ac.cn).

Received 12 November 2007; accepted 10 March 2008; published online 6 April 2008; doi:10.1038/nn.2107

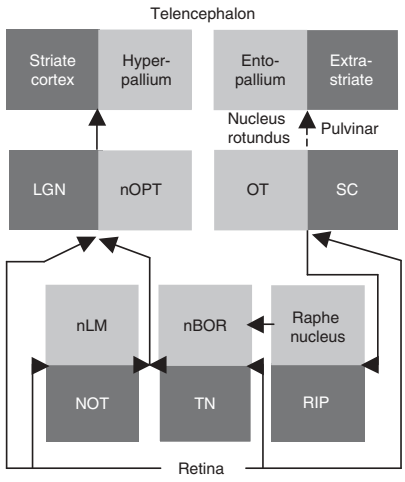

Figure 1 Visual structures and pathways are similar in birds and mammals. Paired squares represent similar structures in birds (light gray) and mammals (dark gray). Arrows symbolize neural projections. In birds, the thalamofugal pathway goes from the nOPT to the telencephalic hyperpallium; the tectofugal pathway projects from the optic tectum (OT) to the nucleus rotundus to the telencephalic entopallium, and the accessory optic pathway projects from the retina to the nBOR. These structures might be homologous to the lateral geniculate nucleus (LGN), striate cortex, superior colliculus (SC), pulvinar, extrastriate cortex and terminal nuclei (TN) of the accessory optic tract in mammals, respectively. The pretectal nLM and the brainstem raphe complex are comparable to the nucleus of the optic tract (NOT) and the nucleus raphe interpositus (RIP), respectively, in mammals. Other abbreviations are defined in the text.

pathways that originate in the saccade-related raphe complex and project through two optokinetic nuclei to nOPT and finally to the telencephalic hyperpallium.

Saccadic responses in telencephalic and thalamic cells

The electro-oculograms (EOG) in **Figure 2** show that a saccade in the pigeon consists of a shift of eye position and several cycles of oscillation[28–30]. When the pigeon faced stationary gratings, its spontaneous saccade had a peak speed of 485 ± 60 deg s^{-1} and a duration of 242 ± 36 ms with 6.4 ± 1.0 cycles of oscillation (mean ± s.d., n = 600). As illustrated in **Figure 2a,c**, the firing rates of all telencephalic neurons recorded began to drop 73 ± 44 ms before saccade onset and underwent an inhibition that lasted 348 ± 50 ms followed by enhanced firing that began at saccade offset and lasted for 385 ± 78 ms (n = 20). Perisaccadic changes in the firing rates of all nOPT cells examined were in phase with those in telencephalic cells. Although the onset times of inhibition and enhancement in nOPT cells preceded those in telencephalic cells by 20–30 ms, the durations of inhibition and enhancement were not different between telencephalic and thalamic cells ($P > 0.60$, n = 20 each).

To evaluate the possibility that perisaccadic inhibition and enhancement in telencephalic cells originate from nOPT cells, we tested the effects of inactivating nOPT on perisaccadic activity in six telencephalic cells that had spontaneous activity (24 ± 11 spikes s^{-1}) and visual responses. When the pigeon made saccades across stationary gratings, the firing rates in these cells began to decrease 67 ± 26 ms before saccade onset. The inhibition lasted 342 ± 65 ms with a change ratio of 43 ± 11% and was followed by enhancement, which started 275 ± 42 ms after saccade onset and lasted for 360 ± 22 ms with a change ratio of 34 ± 9%. Saccadic inhibition and enhancement in all six cells were completely abolished 1–5 min after GABA was injected into the nOPT and recovered in 5–10 min (**Supplementary Fig. 1** online). The spontaneous firing of these telencephalic cells was reduced by ~20% during nOPT blockade.

We then examined saccadic responses in nOPT cells under different conditions. When the pigeon made saccades across stationary gratings, saccadic inhibition and enhancement in nOPT cells lasted 340 ± 45 ms and 388 ± 96 ms, respectively (n = 20, **Fig. 2a,c**). The perisaccadic responses persisted when saccades were made across a blank screen (n = 20, duration = 340 ± 70 ms for inhibition and 395 ± 72 ms for enhancement) and during saccades in complete darkness (n = 20, duration = 345 ± 54 ms for inhibition and 393 ± 65 ms for enhancement). One-way ANOVA analysis indicated that the durations of saccadic inhibition ($F_{2, 57}$ = 0.05, P = 0.95) and enhancement ($F_{2, 57}$ = 0.05, P = 0.95) in nOPT cells were not different under the three visual conditions. The change ratios of firing rates were 52 ± 15% for inhibition and 61 ± 18% for enhancement during saccades across stationary gratings, 55 ± 11% and 62 ± 18% during saccades across a blank screen and 54 ± 19% and 64 ± 21% during saccades in complete darkness. The magnitudes of inhibition ($F_{2, 57}$ = 0.13, P = 0.88) and enhancement ($F_{2, 57}$ = 0.17, P = 0.84) in nOPT cells were also not different under the three conditions, even though there were some small differences in spontaneous firing rates.

During the slow phase of OKN that is induced by the motion of the gratings, the firing rates of telencephalic and nOPT cells were enhanced relative to those during steady fixation. However, saccades in the form of the quick phase of OKN were accompanied by inhibition and

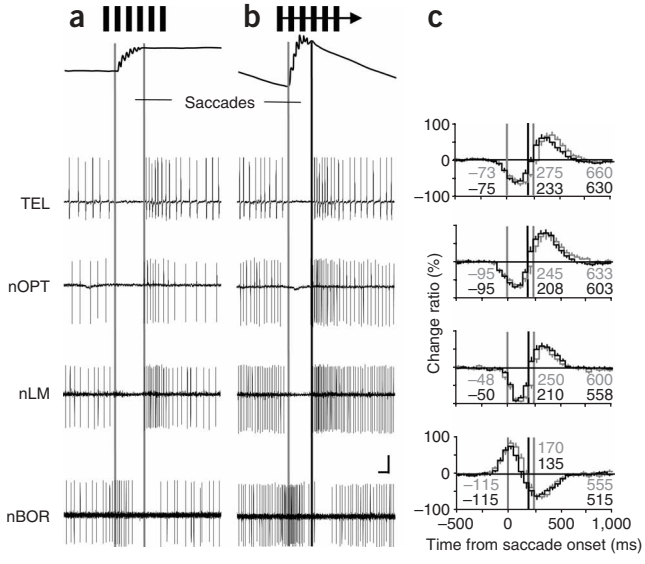

Figure 2 Firing patterns and time course of responses in visual neurons in four brain regions during spontaneous saccades and OKN. (**a**,**b**) Five rows of traces (from top to bottom) show eye movements measured with EOG and saccadic responses of single neurons in the telencephalic hyperpallium (TEL), nOPT, nLM and nBOR during spontaneous saccades made by the pigeon viewing stationary gratings (**a**) and the quick phase of OKN induced by motion (arrow) of the gratings (**b**). (**c**) Time course of the change ratio of firing rates before, during and after spontaneous (light gray) and optokinetic (dark gray) saccades. Numerals (from left to right) give the start time for the first component and the end time for the first and second components of the inhibition and enhancement, respectively. Data show averages for 20 neurons in each corresponding structure. Error bars, s.e.m. Vertical lines limit saccadic duration. Scale bars at the bottom-right of **b** represent 100 ms, 25 μV.

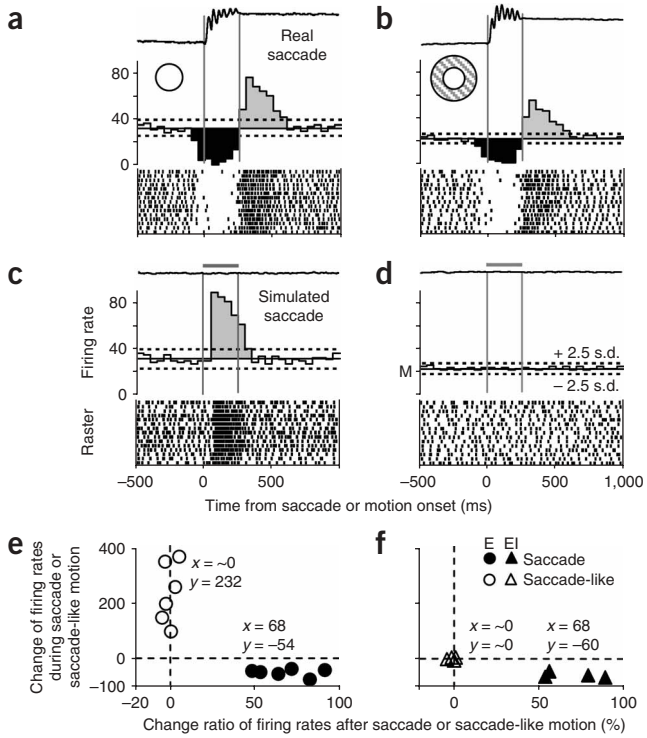

Figure 3 Comparisons of responses of nOPT neurons during saccades across stationary gratings and simulated saccade-like motion of gratings. (**a**–**d**) Responses of two neurons (**a**,**c** and **b**,**d**). From top to bottom, each panel shows an example EOG trace, histograms of average firing rate obtained from 15 saccades or stimuli and a raster display showing individual responses. When tested with small hand-held stimuli and large field gratings for the properties of the visual receptive fields, the neuron in panels **a** and **c** had a purely excitatory field (open circle in **a**), whereas the neuron in panels **b** and **d** had excitatory-inhibitory fields (concentric circles in **b**). The absence of an eye movement is shown by EOG traces at the top of panels **c** and **d**, with horizontal short bars indicating the duration of simulated saccade-like motion. Vertical lines indicate the onset and offset of real (**a**,**b**) or simulated saccade-like motion (**c**,**d**). Letter M in **d** represents mean spontaneous rate. (**e**,**f**) Quantitative summary of responses in six neurons (E) with excitatory (**e**) and four (EI) with excitatory-inhibitory (**f**) receptive fields. Graphs plot the change ratio during a saccade as a function of that after the saccade. Filled and open symbols show responses to real or simulated saccades, respectively.

enhancement of firing rates that were very similar to those seen in the same neurons during spontaneous saccades (**Fig. 2a**,**b**). The parameters of saccades and the neural responses depended weakly on whether the saccades were part of OKN or spontaneous. The average saccade duration was reduced from 242 ± 36 ms for spontaneous saccades to 204 ± 33 ms ($n = 600$) for optokinetic saccades, and the duration of inhibition of firing rates in telencephalic and thalamic cells ($n = 20$ each) was reduced by ~40 ms. However, the duration of enhancement in these cells was the same during spontaneous and optokinetic saccades. Thus, comparison of responses for these neurons revealed more similarities than differences in the responses for spontaneous saccades versus optokinetic ones (**Fig. 2c**). The insensitivity of saccadic responses of nOPT cells to the four visual conditions (stationary and moving gratings, blank screen, and darkness) implies that saccadic responses originate from central structures rather than from retinal image motion.

To further test whether the perisaccadic modulation of firing activity originates from the visual smear of retinal images during saccades, we compared the responses of 10 nOPT cells to saccades across stationary gratings with their responses to simulated saccades (oscillatory gratings (25 Hz) that were moved at a saccade-like speed (480 deg s^{-1}) for the saccadic duration (240 ms) while the eyes were stationary, as identified by steady EOG signals). All ten cells showed typical sequences of inhibition followed by enhancement of firing rates during and after real saccades (**Fig. 3a**,**b**), but each responded to simulated saccades depending on its receptive field organization (**Fig. 3c**,**d**), as mapped previously[14]. We observed that six of the cells (60%) increased their firing rates in response to simulated saccades during fixation (**Fig. 3c**,**e**). The same cells responded to both large-field gratings and a hand-held target, and were thus characterized by a single excitatory receptive field. Another four cells (40%) responded to the motion of a small target, but not to the motion of large-field gratings, indicating that they had concentric excitatory and inhibitory receptive fields. The balanced combination of excitatory and inhibitory subunits in the receptive fields of the latter neurons explained the lack of responses to simulated saccade-like motion of gratings when the eyes were stationary (**Fig. 3d**,**f**). In no case did the response of a nOPT cell during simulated saccades show any sign of the strong inhibition seen during real saccades.

Optokinetic origin of saccadic responses in nOPT cells

We next evaluated the pattern of synaptic connections to nOPT cells from the optokinetic nuclei. Saccadic inhibition and enhancement of firing rates in nLM neurons paralleled those in the nOPT (**Fig. 2**). The inhibition began 48 ± 38 ms before saccade onset and lasted for 298 ± 50 ms ($n = 20$) until saccade offset and then was followed by enhancement lasting 350 ± 58 ms (**Fig. 2a**,**c**). By contrast, nBOR cells showed saccadic responses with the opposite phase. Firing was enhanced from 115 ± 49 ms before saccade onset and then inhibited from 170 ± 50 ms ($n = 20$) after saccade onset for 385 ± 69 ms (**Fig. 2a**,**c**). The change ratio for saccadic inhibition and enhancement in these cells was 50–60%. Similar to nOPT cells, the firing rates of nLM and nBOR cells during the slow phase of OKN were enhanced in comparison with the firing rates during steady fixation, and their response patterns during the quick phase of OKN were similar to those during spontaneous saccades, with the durations of inhibition in nLM cells and enhancement in nBOR cells being reduced by 35–40 ms ($n =$ 20 in each sample; **Fig. 2b**,**c**).

The saccadic responses of nLM cells are in phase and those of nBOR cells are out of phase with the saccadic responses of nOPT cells; the nLM-nOPT pathway is excitatory whereas the nBOR-nOPT pathway is inhibitory[14]. These facts indicate that the inputs from the nBOR and nLM might work together to reciprocally modulate the responses of nOPT cells during saccades. To evaluate this possibility, we examined the effects of reversible inactivation of the nBOR, nLM or both on the saccadic responses of nOPT cells (**Fig. 4**). Blockade of nBOR using GABA reduced the change ratio for saccadic inhibition and enhancement, respectively, in 12 nOPT cells by 57% and 52% of control values, and delayed inhibition onset to 42 ms, rather than 100 ms before saccade onset. There was no change in enhancement onset (242 versus 238 ms; **Fig. 4a**,**d**,**g**). The reduced inhibition latency is expected because the nBOR-nOPT pathway is inhibitory[14] and the saccadic responses of nBOR cells are out of phase with those of nOPT cells (**Fig. 2**); eliminating the enhancement and inhibition of nBOR responses should reduce the inhibition and enhancement of nOPT responses. On the other hand, blockade of the nLM reduced the change ratio for saccadic inhibition and enhancement in an additional 12 nOPT cells by 43% and 45% of control values, respectively. The onset of enhancement in these cells was advanced from 258 to 196 ms after saccade onset, and

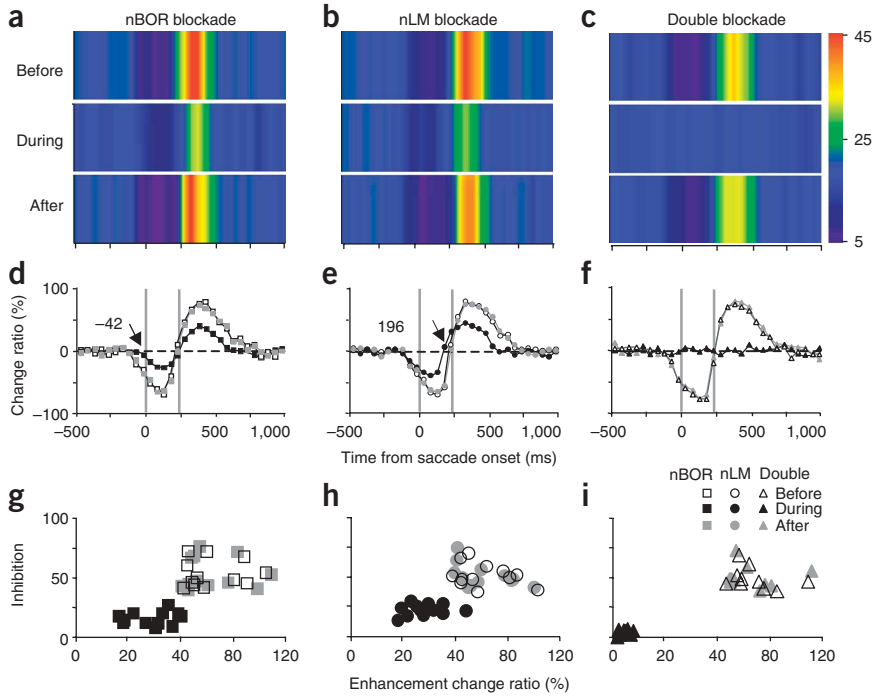

Figure 4 Effects of blockade of the optokinetic nuclei by GABA on saccadic responses of nOPT neurons. From left to right, the three columns show data for inactivation of the nBOR, nLM or both. Top row, firing rates of three nOPT cells (**a**–**c**) before, during and after blockade are color-coded with a scale (spikes per s) on the right. Middle row, time course of the change ratio of nOPT cells ($n = 12$ in **d**,**e**; 10 in **f**). Arrows point to the onset of delayed inhibition (**d**) or advanced enhancement (**e**) during blockade. Bottom row, quantitative summary of results from the full sample of nOPT neurons (**g**–**i**). Each graph plots the absolute value of the change ratio for inhibition as a function of that for enhancement. Open, filled and gray symbols show data before, during and after blockade, respectively.

the onset of inhibition did not change (92 versus 96 ms; **Fig. 4b**,**e**,**h**). This reduction is also expected because the nLM-nOPT pathway is excitatory[14] and the saccadic responses of nLM cells are in phase with those of nOPT cells (**Fig. 2**): eliminating the inhibition followed by enhancement of nLM responses should reduce the inhibition and enhancement of nOPT responses. Finally, simultaneous application of GABA to both the nBOR and the nLM resulted in total elimination of saccadic responses in nOPT cells ($n = 10$; **Fig. 4c**,**f**,**i**). In all cases, responses returned to control levels after time had been allowed for the injected GABA to be cleared. These results were confirmed by the loss of saccadic responses in nOPT cells ($n = 12$) after electrolytic lesions of both nBOR and nLM (**Fig. 5**). It is noteworthy that the pathway from the retina to the nOPT was intact while the nBOR or nLM was inactivated, indicating that changes in saccadic responses of nOPT cells under these circumstances were caused by contributions of the optokinetic nuclei. It seems that both nBOR and nLM are necessary for the saccadic responses of nOPT cells and that the retina-nOPT pathway is not sufficient. Further studies indicated that the saccadic responses of optokinetic neurons are in turn modulated by the saccade-related raphe complex.

Two types of omnipause cells modulate optokinetic cells

The brainstem reticular formation contains omnipause neurons (OPNs) that are active at high rates during fixation and pause firing before and during saccades in all directions[23,26,31]. We recorded 49 cells from the brainstem raphe complex, all of which paused firing during spontaneous saccades in multiple directions and during optokinetic saccades induced by motion of gratings in the four cardinal directions. Analysis of the timing of onset and offset of the pauses divided the raphe neurons into two groups (**Fig. 6**). Early OPNs (53%) stopped firing 133 ± 37 ms before saccade onset and recovered 72 ± 57 ms before saccade offset ($n = 20$, **Fig. 6a**,**c**), and late OPNs (47%) paused 77 ± 14 ms before saccade onset and recovered 400 ± 89 ms after saccade offset ($n = 20$, **Fig. 6a**,**c**). The qualitative difference in the responses of the two groups of OPNs can be seen in the example perisaccadic histograms of **Figure 6a**.

Antidromic stimulation of the nBOR and nLM revealed that the two groups of OPNs projected differently. Stimulation of the nBOR evoked spikes in six of ten early OPNs with latencies of 2.2 ± 1.0 ms, but did not evoke spikes in any of the ten late OPNs examined (**Fig. 6b**,**c**). By contrast, nLM stimulation evoked spikes in eight of ten late OPNs with latencies of 5.4 ± 1.2 ms, but did not evoke spikes in any of the ten early OPNs examined (**Fig. 6b**,**c**). Electrical stimulation of the raphe complex revealed the signs of raphe projections to the optokinetic nuclei (**Fig. 7**). Raphe stimulation decreased firing activity in all the 15 nBOR cells examined. The latencies of inhibitory responses were bimodal: short-latency and long-latency groups had latencies of 2.9 ± 0.5 ms ($n = 5$) and 19.0 ± 4.8 ms ($n = 10$), respectively. The raphe-nBOR inhibition lasted 19.6 ± 14.3 ms ($n = 15$) and was not different in

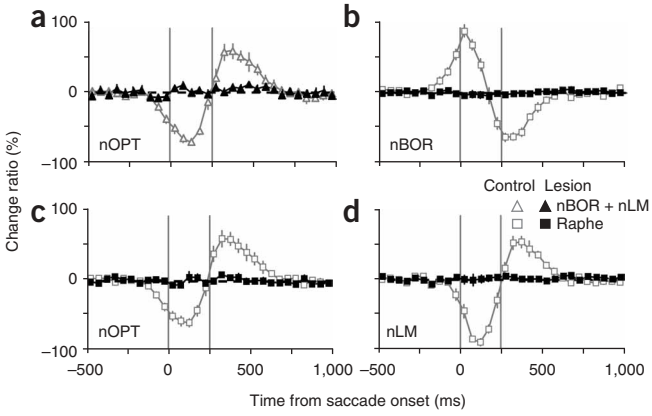

Figure 5 Effects of optokinetic or raphe lesions on saccadic responses of thalamic and optokinetic neurons. (**a**) Electrolytic lesions of both optokinetic nuclei nBOR and nLM abolished saccadic responses in nOPT cells ($n = 12$). (**b**–**d**) Electrolytic lesions of the raphe complex eliminated saccadic responses in nOPT, nBOR and nLM cells ($n = 12$ in each sample). Each graph plots the change ratio of firing rates as a function of the time from saccade onset. Negative values on the *x* axis indicate the time before saccade onset; negative values on the *y* axis indicate a reduction in firing. Open and filled symbols show responses measured before or after the lesions (**Supplementary Fig. 2**). Vertical lines delimit saccadic duration. Error bars represent s.e.m.; time bin represents 50 ms.

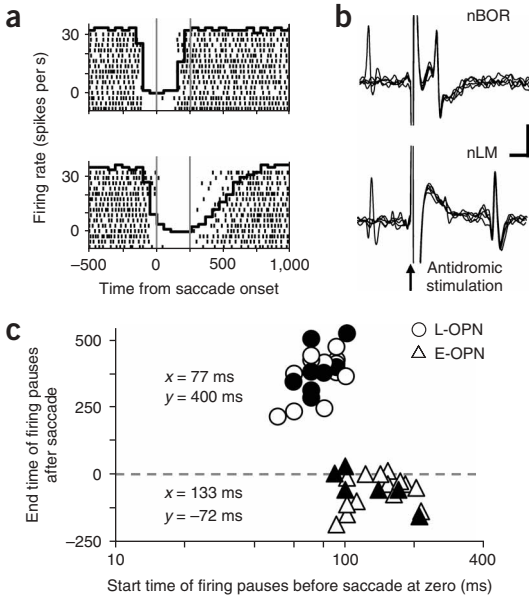

Figure 6 Classification of raphe neurons and their responses to antidromic stimulation of the optokinetic nuclei. (**a**) Superimposed histograms and rasters for raphe neurons that started and ended perisaccadic pauses early (top, E-OPN) and late (bottom, L-OPN) relative to the saccade. The rasters and histograms show responses accumulated across 15 spontaneous saccades in multiple directions. (**b**) Antidromic spikes in the cell shown in the top panel of **a** evoked by nBOR stimulation (top) and those in the cell shown in the bottom panel of **a** by nLM stimulation (bottom). Five traces are superimposed. Scale bars represent 50 μV, 1 ms. (**c**) Summary of response latencies for 20 E-OPNs (triangles) and 20 L-OPNs (circles). Filled triangles and circles show 6 E-OPNs and 8 L-OPNs that were activated antidromically from the nBOR or nLM. The start time before saccade onset is plotted on a log scale.

duration between groups (**Fig. 7a**,**c**). Raphe stimulation increased activity in all 15 nLM cells, again with bimodal latencies. The two groups of nLM cells had latencies of 5.8 ± 1.3 ms ($n = 4$) and 32.7 ± 9.0 ms ($n = 11$). The raphe-nLM excitation lasted 15.5 ± 5.3 ms for the short-latency group and 45.9 ± 19.7 ms for the long-latency group (**Fig. 7b**,**d**). We found no topographic organization in the raphe-nLM and raphe-nBOR projections, and both long-latency and short-latency responses in the nBOR or nLM could be elicited by raphe stimulation at single sites.

Finally, we examined the effects of inactivating the raphe complex on saccadic responses in thalamic and optokinetic neurons. Electrolytic lesions of the raphe complex caused normal saccades to be replaced by slow shifts of the eyes, which could be generated by the intact optokinetic nuclei. Alignment of neural responses by shift onset showed that raphe lesions resulted in complete elimination of saccadic responses in all nBOR, nLM and nOPT cells examined ($n = 12$ each; **Fig. 5b–d**), yielding effects similar to those obtained by raphe lesions with kainic acid (two pigeons, five cells; t-test, $n_1 = 12$, $n_2 = 5$, $t = 1.19$, $P = 0.25$). Moreover, the saccadic responses of nOPT cells ($n = 12$) after raphe inactivation were statistically identical to those after electrolytic lesions of both the nBOR and the nLM ($n = 12$, **Fig. 5a**) (t-test, $n = 12$, $t = 0.43$, $P = 0.67$) and simultaneous inactivation of both optokinetic nuclei by GABA ($n = 10$, **Fig. 4c**,**f**,**i**; t-test, $n_1 = 12$, $n_2 = 10$, $t = 1.44$, $P = 0.16$). We conclude that raphe neurons send corollary discharge signals to nOPT neurons through both optokinetic nuclei.

Histological verification

Fifty-five electrode sites marked were all localized in the telencephalic hyperpallium (4), nOPT (15), nBOR (13), nLM (14) and raphe complex (9). In addition, the raphe complex in five pigeons and both optokinetic nuclei in three pigeons were lesioned at the correct places (**Supplementary Fig. 2** online). These marks validate the stereotaxic coordinates we used and provide anatomical support for our conclusions.

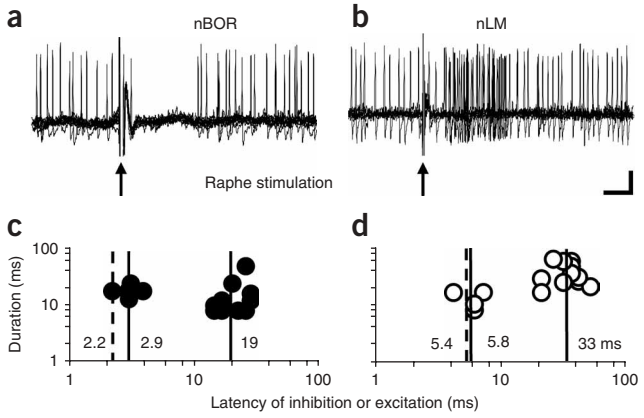

Figure 7 Responses of neurons in the nBOR and nLM to electrical stimulation of the raphe complex. (**a**,**b**) Original recordings show that a neuron in the nBOR was inhibited by raphe stimulation and one in the nLM was excited by stimulation of the raphe complex. Ten repeats were accumulated. Scales: 50 μV, 10 ms. (**c**,**d**) The duration of responses evoked in 15 nBOR (filled circles) and 15 nLM (open circles) cells by raphe stimulation are plotted on a log scale against response latencies also plotted on a log scale. Average latencies for orthodromic stimulation of the raphe complex and antidromic stimulation of the optokinetic nuclei are expressed in numerals beside solid and dashed vertical lines, respectively.

DISCUSSION

Our study provides several lines of evidence that saccadic inhibition and facilitation of telencephalic neurons in birds are driven by corollary discharge signals, and elucidated the pathways for transmitting the signals from the raphe complex through the optokinetic nuclei to the thalamus and then to the hyperpallium. **Figure 8** summarizes these physiological and anatomical results. To our knowledge, this is the first demonstration of a neural circuit mechanism for the mediation by corollary discharge of a profound perisaccadic modulation of firing activity in telencephalic neurons, although previous studies have described a different corollary discharge circuit from the superior colliculus to the frontal eye fields[3,12].

We demonstrated the full pathway for corollary discharge from the OPN in the raphe complex to the telencephalic hyperpallium, the avian homolog of the visual cortex. Telencephalic cells receive inputs from the nOPT[32–34] and their saccadic responses originate from the nOPT, because these responses are eliminated by inactivation of the nOPT. The saccadic responses of nOPT cells are identical under different visual conditions, proving that they do not depend on visual input[6,7]. On the other hand, saccade-like motion of gratings does not produce such saccadic responses but instead causes different visual responses only. All this indicates that the profound effect of saccades on the responses of pigeon visual neurons originates from central but not retinal sources. Because the saccadic responses of nOPT cells are in phase with those in nLM cells and out of phase with those in nBOR

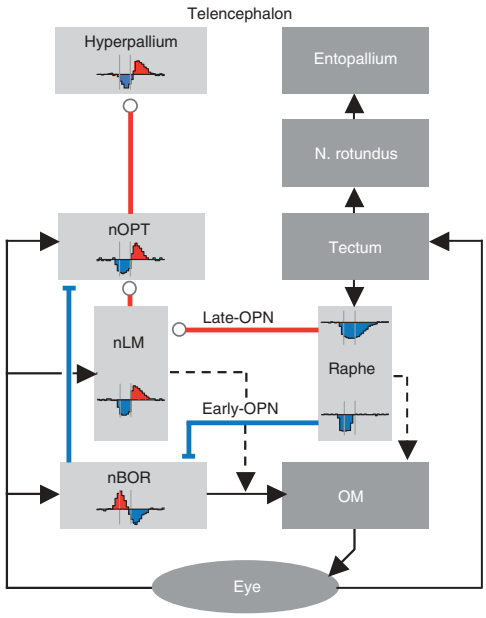

Figure 8 Summary diagram showing neuronal pathways and information flow related to saccadic responses in the structures under study (light gray rectangles; dark gray represents structures not studied here). Visual neurons in the telencephalic hyperpallium receive input from the nOPT, which in turn receives excitatory input from the nLM and inhibitory input from the nBOR. Meanwhile, the nLM receives excitatory input from the late omnipause neurons (OPN) and the nBOR receives inhibitory input from the early omnipause neurons in the raphe complex. Dashed lines represent neuronal pathways identified in mammals[26,36] but not yet identified in the pigeon from the pretectum and the brainstem reticular formation to the oculomotor nuclei (OM). Histograms show saccadic inhibition and enhancement of single cells in their respective structures (15 repeats, time bin = 50 ms). Vertical lines in histograms delimit saccadic duration. Excitatory pathways or enhancement in histograms is shown in red and inhibitory pathways or inhibition in blue.

cells, and because the nLM-nOPT pathway is excitatory and the nBOR-nOPT pathway is inhibitory[14], inactivation of either nLM or nBOR alone causes a 50% reduction of saccadic responses in nOPT cells, whereas simultaneous inactivation of both optokinetic nuclei eliminates thalamic perisaccadic responses.

The motor system origin of the saccadic responses of optokinetic neurons seems to be the raphe complex. Omnipause neurons in the pigeon's raphe complex behave like those found in the primate nucleus raphe interpositus[23,26,31] but could be divided into early OPN and late OPN groups. The former send inhibitory signals to nBOR and the latter excitatory ones to nLM, thereby enhancing nBOR activity and reducing nLM activity perisaccadically. Although we do not know the origin of the post-saccadic inhibition in the nBOR and enhancement in the nLM and nOPT, the total elimination of saccadic responses in nOPT neurons by inactivation of the nLM and nBOR (and in optokinetic cells by raphe lesions) implies that the second component of each response, like the first, arises from corollary discharge. It seems that the pathway from the raphe to the nOPT through the nBOR contains two inhibitory synapses whereas that relayed by the nLM contains two excitatory synapses, indicating that corollary discharge signals related to saccades are sent in parallel through both optokinetic nuclei to the nOPT and then to the telencephalon.

Important support for the idea that the saccadic responses reported here originate from corollary discharge comes from the fact that they begin before saccade onset in all the five brain areas we surveyed. Furthermore, the timing of saccadic responses in the raphe, nBOR, nLM, nOPT and telencephalon strongly supports the notion that the signals that initiate saccadic responses in telencephalic neurons originate from the motor commands of eye movements and proceed through the chain of pathways shown in **Figure 8**. Firing in early OPNs and late OPNs begins to pause 133 ms and 77 ms before saccade onset, respectively. These time courses lead to enhancement of nBOR activity that begins 115 ms before saccade onset and inhibition of nLM activity that begins 48 ms before saccade onset. The signals for enhancement and inhibition transmitted through the nBOR- and nLM-thalamic pathways would initiate inhibition in nOPT cells that starts 95 ms before saccade onset and lasts until the end of the saccade. Then, inhibition in nOPT cells would initiate inhibition in telencephalic cells 73 ms before saccade onset. It seems that optokinetic and raphe neurons send motor commands to the oculomotor nuclei[35,36] and 'efference copies' to nOPT cells, whose saccadic responses initiate those in telencephalic cells. This dual signaling could be accomplished by two groups of motor neurons with one projecting to the oculomotor nuclei and the other to nOPT. Alternatively, the axons of optokinetic and raphe neurons could bifurcate and send their collaterals to different regions.

We found good agreement between the latencies of the various neural pathways and the effects of lesions on the timing of residual perisaccadic responses. Comparison of **Figures 2** and **4** indicates that blockade of the nBOR delays the inhibition onset of nOPT cells to 42 ms before saccades, implying that the signal for nLM inhibition onset at 48 ms would take 6 ms to reach the nOPT through the excitatory pathway, in agreement with the time for nLM-nOPT transmission[14]. In contrast, blockade of the nLM advances the enhancement onset of nOPT cells to 196 ms, implying that the signal for nBOR inhibition onset at 170 ms would take 26 ms to reach the nOPT through the inhibitory pathway as taken by nBOR-nOPT transmission[14]. It is clear that saccadic responses of the nOPT are modulated by both optokinetic nuclei.

The pigeon is an excellent model in which to describe the neural pathways for modulation of the responses of visual neurons by a corollary discharge related to saccades in multiple directions. We expect that similar corollary discharge pathways exist in mammals and that they mediate many of the perceptual and motor sequelae to saccades. Indeed, many studies in mammals postulate that corollary discharges from the motor system are important in sensory and motor processing. For example, the spatial accuracy of saccades and visual processing depends on corollary discharge pathways from the superior colliculus through the thalamus to the frontal eye fields[3,12], and accurate sustained pursuit eye movements depend on corollary discharge pathways between the brainstem and cerebellar flocculus[37]. It is also likely that the enhancement of cortical activity is involved in the post-saccadic facilitation of visual processing, as seen during smooth pursuit eye movements in primates[8,38,39]. It must also contribute to the remapping of cortical receptive fields to maintain an accurate retinal representation when saccades occur and to the spatial and temporal distortions that occur around saccades. The saccadic effects on pursuit seem to be driven by omnidirectional corollary discharge signals like those shown here, whereas the directional nature of the signals that drive spatial and temporal distortions remain unclear.

Analysis of the neural basis for these behaviors is better done in primates, but we think that the complete corollary discharge circuit we discovered in the pigeon should provide a basis for identifying the mechanisms of behaviors that rely on corollary discharge in primates. Although it remains controversial, there is some evidence in primates

for effects of corollary discharge on neurons in the visual pathways. For example, neurons in both the visual cortex[9,10] and LGN[6,7] show reduction followed by enhancement of firing rates perisaccadically. The LGN of mammals receives inputs from the pretectum[36,40–42] and from the dorsal terminal nucleus of the accessory optic tract[40]. On this basis, we expect that the same kinds of perisaccadic modulation we found in all pigeon visual neurons will be present in a subset of mammalian visual neurons, and that it will prove to have important functions for behaviors that depend on corollary discharge related to the execution of saccades.

METHODS

Preparation and setup. The experiments were carried out on 70 pigeons (*Columba livia*) of either sex and 300–450 g body weight, and complied with the guidelines for the care and use of animals established by the Society for Neuroscience and approved by the Institutional Animal Administration Committee. Each pigeon was anesthetized by injection of ketamine (40 mg kg^{-1}) and xylazine (5 mg kg^{-1}) into pectoral muscles, and the depth of anesthesia was monitored by breathing patterns and by the reflex from pinching the toe. The pigeon was placed in a stereotaxic apparatus and its scalp was incised and retracted, and the left tectum, telencephalon and/or cerebellum were exposed with a dental drill and surgical forceps. A lightweight steel headpiece connected to a steel rod was cemented onto the skull to replace the ear bars as a means to fix the pigeon's head. After the opening in the scalp was closed and treated with erythromycin ointment, the pigeon was given ibuprofen as an analgesic (20 mg kg^{-1}) for postoperative pain and returned to its home cage to recover from anesthesia. In 10–12 h, the pigeon's standing, walking and pecking behaviors had returned to normal. It then was lightly anesthetized with ketamine, wrapped in a bag and placed on a foam couch. The headpiece was reconnected to the rod for stereotaxic fixation. The scalp was retracted again and the dura mater overlying the telencephalic hyperpallium, nOPT, nLM, nBOR and/or raphe complex was excised. The wound edge and muscles were periodically infiltrated with lidocaine. The left eye was covered but allowed to move freely, and the right eye was held open during recording. A screen of 130° by 140° was placed 40 cm away from the viewing eye. The horizontal axis of the visual field on the screen was rotated by 38° to match the pigeon's normal conditions[30,43]. The pigeon's adaptation to the restraint was signaled by the observation that it sat unruffled in the apparatus in 2 h. Then, both single-cell activity and EOG were recorded simultaneously.

Visual conditions. A large square-wave grating consisting of equal-width black and white stripes with spatial frequencies of 0.08 or 0.5 cycles per deg was generated by a computer with graphics GeForce 7950 (maximum refresh rate 400 Hz, Nvidia) and rear-projected onto the screen by a projector (maximum refresh rate 200 Hz, XG-C58X, Sharp). The refresh rate of 200 Hz of the display system was verified with a photoelectric device (Si photodiode S1227-33BQ, Hamamatsu Photonics) and an oscilloscope (54622A, Agilent Technologies). The luminances of black and white in the grating were 0.1 and 6.6 cd m^{-2}, respectively. The responses of neurons were recorded during spontaneous saccades emitted while the pigeon viewed stationary gratings, a blank screen that was uniformly illuminated (6.6 cd m^{-2}) and featureless to human observers and complete darkness (1.9×10^{-6} lux, RTR Optoelectronics Technology). Some neurons were also examined for responses to simulated saccade-like motion of gratings (0.08 cycles per deg; velocity, 480° s^{-1}; duration, 240 ms; oscillation frequency, 25 Hz) while the viewing eye was stationary as identified by steady EOG signals. In other experiments, gratings of 0.5 cycles per deg were moved at 2–16° s^{-1} in the temporo-nasal direction to elicit OKN for comparison of neuronal responses to spontaneous and optokinetic saccades. Eye movements were monitored by EOG for all visual conditions. The interval between consecutive trials was 20 s to allow neuronal responses to recover fully from any adaptation.

Electrodes and recording. We used four types of electrode. The first was a single micropipette (~2-μm tip diameter) filled with 2 M sodium acetate, and 2% (wt/vol) pontamine skyblue was used for extracellular recording and making marks. Spikes were amplified, displayed and stored in a digital data recorder (RD-135T, TEAC) for off-line analysis. Some recording sites were marked as described[30,43]. The second electrode was a two-barrel micropipette that we used for blocking the nOPT, nBOR and/or nLM, or raphe complex; one barrel was filled as above and used to confirm the electrode location physiologically and anatomically, and the other barrel contained GABA (100 mM, pH 3.3) or kainic acid (9.4 mM, pH 7.4, Sigma Chemical) and was connected to a pneumatic picopump (PV800, WPI) for applying GABA (80–120 nl) or kainic acid (200–300 nl)[14,17]. The third electrode was a tungsten bipolar electrode that we used for electrical stimulation of the nLM, nBOR or raphe complex. Its poles were separated by 400 μm[14,44] and were glass-coated with 60 μm of tip exposed. The fourth electrode type that we used were three steel electrodes (27-gauge syringe needles) for recording EOG, with two inserted into the anterior and posterior regions of the right orbital arch and one as reference in the occipital bone[29]. In some experiments, two additional needles were placed above and beneath the orbit to record eye movements in vertical directions. EOG signals were amplified (DC to 200 Hz) and stored for off-line analysis with neuronal spike data.

All microelectrodes were advanced into brain structures according to the pigeon brain atlas[45]. When we examined the effects of the nLM and/or nBOR on a nOPT cell, we injected GABA at up to three sites in the nBOR (A4.5–4.0, L1.8, H4.0) and/or nLM (A5.7, L4.0, H4.5–5.5) to allow us to find a correct site where GABA could block the activity of optokinetic cells projecting to the nOPT cell. Because the nOPT projects topographically to the telencephalic hyperpallium[32,34], injections of GABA (80–120 nl) in the nOPT (A6.5–7.0, L2.8–3.2, H7.0) could influence firing activity in telencephalic cells in a topographic region (A12.0–13.0, L2.0, H11.0–13.0).

Stimulation and lesions. For stimulation with rectangular pulses of 300–500-μA intensity and 50–100-μs duration, a tungsten bipolar electrode was vertically inserted into the nBOR with its poles in a rostrocaudal arrangement to avoid stimulating the optic tract nearby[14] or into the raphe complex (A0.5–P0.5, L0.0, H2.0–3.0). Its poles were arranged dorsoventrally and inserted laterally into the nLM to avoid stimulating the tectum[14]. To create electrolytic lesions by passing positive currents of 300 μA for 10 s, we inserted the bipolar electrode into the nBOR, nLM or raphe complex to make up to three lesions because of their large size and irregular shape. Similar to injection of GABA, kainic acid (200–300 nl) was injected into three sites in the raphe complex for 30–40 min to make chemical lesions. Recordings were made from the pigeons with chemical lesions after 5 d of survival.

At the end of experiments, each of the pigeons was euthanized by intraperitoneal injection of an overdose of urethane (4 g kg^{-1}). For those pigeons with a mark or lesion, the brains were removed from the skull and histologically processed for subsequent microscopic observations of marked and lesioned sites[30,43].

Data analysis. Spike data and eye positions were sampled at 8,000 Hz around each saccade. Spikes were collected from 500 ms before to 1,000 ms after the saccade for data analysis; spikes collected in the interval from 200–500 ms before the saccade were averaged as a control. A saccade was used for data analysis only if it was separated from the previous saccade by at least 1.5 s to avoid an overlap of enhancement (inhibition) induced by the previous saccade, although this probability was negligible (**Fig. 2c**). The onset and offset of a saccade were determined with Cool Edit (Syntrillium Software) according to their characteristic oscillations. For calibration purposes, eye movements were videographed by an infrared video camera (DCR-HC40E, Sony) simultaneously with EOG recordings. The video images were used to calibrate EOG[29], revealing a sensitivity of 62–83 μV per deg.

Spikes were collected before, during and after reversible inactivation, or before and after lesions of the nOPT, nBOR and nLM or raphe complex for 15–30 repeats. Firing rates were averaged in 50-ms bins in each trial. We considered firing rate to be reduced or enhanced during saccades if it was lower or higher than the control rate by more than 2.5 standard deviations. To normalize changes in the responses of different cells, we calculated the change ratio of firing rates, defined as $R = \frac{f_2 - f_1}{f_1}$, where f_1 is the intersaccadic firing rate as control and f_2 is the firing rate during saccades.

Note: Supplementary information is available on the Nature Neuroscience website.

ACKNOWLEDGMENTS

We thank S.G. Lisberger of University of California San Francisco for help in editing the manuscript. This work was supported by the National Natural Science Foundation of China (90208008) and by the Chinese Academy of Sciences (KSCX1-YW-R-32 and Brain-Mind Project).

AUTHOR CONTRIBUTIONS

Yan Yang conducted the experiments throughout, P.C. conducted the first half of the experiments, Yang Yang conducted the second half of the experiments and S.-R.W. supervised the project and wrote the manuscript. All co-authors conducted the data analyses.

Published online at http://www.nature.com/natureneuroscience
Reprints and permissions information is available online at http://npg.nature.com/reprintsandpermissions

1. Tolias, A.S. *et al.* Eye movements modulate visual receptive fields of V4 neurons. *Neuron* **29**, 757–767 (2001).
2. Kusunoki, M. & Goldberg, M.E. The time course of perisaccadic receptive field shifts in the lateral intraparietal area of the monkey. *J. Neurophysiol.* **89**, 1519–1527 (2003).
3. Sommer, M.A. & Wurtz, R.H. Influence of the thalamus on spatial visual processing in frontal cortex. *Nature* **444**, 374–377 (2006).
4. Yarrow, K., Haggard, P., Heal, R., Brown, P. & Rothwell, J.C. Illusory perceptions of space and time preserve cross-saccadic perceptual continuity. *Nature* **414**, 302–305 (2001).
5. Morrone, M.C., Ross, J. & Burr, D. Saccadic eye movements cause compression of time as well as space. *Nat. Neurosci.* **8**, 950–954 (2005).
6. Lee, D. & Malpeli, J.G. Effects of saccades on the activity of neurons in the cat lateral geniculate nucleus. *J. Neurophysiol.* **79**, 922–936 (1998).
7. Reppas, J.B., Usrey, W.M. & Reid, R.C. Saccadic eye movements modulate visual responses in the lateral geniculate nucleus. *Neuron* **35**, 961–974 (2002).
8. Royal, D.W., Sary, G., Schall, J.D. & Casagrande, V.A. Correlates of motor planning and postsaccadic fixation in the macaque monkey lateral geniculate nucleus. *Exp. Brain Res.* **168**, 62–75 (2006).
9. Burr, D.C., Morrone, M.C. & Ross, J. Selective suppression of the magnocellular visual pathway during saccadic eye movements. *Nature* **371**, 511–513 (1994).
10. Ross, J., Burr, D.C. & Morrone, M.C. Suppression of the magnocellular pathways during saccades. *Behav. Brain Res.* **80**, 1–8 (1996).
11. Thiele, A., Henning, P., Kubischik, M. & Hoffmann, K.P. Neural mechanisms of saccadic suppression. *Science* **295**, 2460–2462 (2002).
12. Wurtz, R.H. & Sommer, M.A. Identifying corollary discharges for movement in the primate brain. *Prog. Brain Res.* **144**, 47–60 (2004).
13. Wylie, D.R., Glover, R.G. & Lau, K.L. Projections from the accessory optic system and pretectum to the dorsolateral thalamus in the pigeon (*Columbia livia*): a study using both anterograde and retrograde tracers. *J. Comp. Neurol.* **391**, 456–469 (1998).
14. Cao, P., Yang, Y., Yang, Y. & Wang, S.R. Differential modulation of thalamic neurons by optokinetic nuclei in the pigeon. *Brain Res.* **1069**, 159–165 (2006).
15. McKenna, O.C. & Wallman, J. Accessory optic system and pretectum of birds: comparisons with those of other vertebrates. *Brain Behav. Evol.* **26**, 91–116 (1985).
16. Shimizu, T. & Bowers, A.N. Visual circuits of the avian telencephalon: evolutionary implications. *Behav. Brain Res.* **98**, 183–191 (1999).
17. Gioanni, H., Rey, J., Villalobos, J., Richard, D. & Dalbera, A. Optokinetic nystagmus in the pigeon (*Columba livia*). II. Role of the pretectal nucleus of the accessory optic system (AOS). *Exp. Brain Res.* **50**, 237–247 (1983).
18. Clement, G. & Magnin, M. Effects of accessory optic system lesions on vestibule-ocular and optokinetic reflexes in the cat. *Exp. Brain Res.* **55**, 49–59 (1984).
19. Schiff, D., Cohen, B., Buttner-Ennever, J. & Matsuo, V. Effects of lesions of the nucleus of the optic tract on optokinetic nystagmus and after-nystagmus in the monkey. *Exp. Brain Res.* **79**, 225–239 (1990).
20. Toledo, C.A., Hamassaki-Britto, D.E. & Britto, L.R. Serotonergic afferents of the pigeon accessory optic nucleus. *Brain Res.* **705**, 341–344 (1995).
21. Reiner, A. & Karten, H.J. Laminar distribution of the cells of origin of the descending tectofugal pathway in the pigeon (*Columba livia*). *J. Comp. Neurol.* **204**, 165–187 (1982).
22. Luksch, H. Cytoarchitecture of the avian optic tectum: neuronal substrate for cellular computation. *Rev. Neurosci.* **14**, 85–106 (2003).
23. Everling, S., Pare, M., Dorris, M.C. & Munoz, D.P. Comparison of the discharge characteristics of brain stem omnipause neurons and superior colliculus fixation neurons in monkey: implications for control of fixation and saccade behavior. *J. Neurophysiol.* **79**, 511–528 (1998).
24. Brecht, M., Singer, W. & Engel, A.K. Amplitude and direction of saccadic eye movements depend on the synchronicity of collicular population activity. *J. Neurophysiol.* **92**, 424–432 (2004).
25. Angeles Luque, M., Perez-Perez, M.P., Herrero, L. & Torres, B. Involvement of the optic tectum and mesencephalic reticular formation in the generation of saccadic eye movements in goldfish. *Brain Res. Brain Res. Rev.* **49**, 388–397 (2005).
26. Sparks, D.L. The brainstem control of saccadic eye movements. *Nat. Rev. Neurosci.* **3**, 952–964 (2002).
27. Horn, A.K. The reticular formation. *Prog. Brain Res.* **151**, 127–155 (2005).
28. Pettigrew, J.D., Wallman, J. & Wildsoet, C.F. Saccadic oscillations facilitate ocular perfusion from the avian pecten. *Nature* **343**, 362–363 (1990).
29. Wohlschläger, A., Jäger, R. & Delius, J.D. Head and eye movements in unrestrained pigeons (*Columba livia*). *J. Comp. Psychol.* **107**, 313–317 (1993).
30. Niu, Y.Q., Xiao, Q., Liu, R.F., Wu, L.Q. & Wang, S.R. Response characteristics of the pigeon's pretectal neurons to illusory contours and motion. *J. Physiol. (Lond.)* **577**, 805–813 (2006).
31. Keller, E.L. Participation of medial pontine reticular formation in eye movement generation in monkey. *J. Neurophysiol.* **37**, 316–332 (1974).
32. Bagnoli, P. & Burkhalter, A. Organization of the afferent projections to the wulst in the pigeon. *J. Comp. Neurol.* **214**, 103–113 (1983).
33. Güntürkün, O. & Karten, H.J. An immunocytochemical analysis of the lateral geniculate complex in the pigeon (*Columba livia*). *J. Comp. Neurol.* **314**, 721–749 (1991).
34. Koshiba, M., Yohda, M. & Nakamura, S. Topological relation of chick thalamofugal visual projections with hyperpallium revealed by three color tracers. *Neurosci. Res.* **52**, 235–242 (2005).
35. Brecha, N. & Karten, H.J. Accessory optic projections upon oculomotor nuclei and vestibulocerebellum. *Science* **203**, 913–916 (1979).
36. Buttner-Ennever, J.A., Cohen, B., Horn, A.K. & Reisine, H. Pretectal projections to the oculomotor complex of the monkey and their role in eye movements. *J. Comp. Neurol.* **366**, 348–359 (1996).
37. Lisberger, S.G. & Fuchs, A.F. Role of primate flocculus during rapid behavioral modification of vestibuloocular reflex. I. Purkinje cell activity during visually guided horizontal smooth-pursuit eye movements and passive head rotation. *J. Neurophysiol.* **41**, 733–763 (1978).
38. Lisberger, S.G. Postsaccadic enhancement of initiation of smooth pursuit eye movements in monkeys. *J. Neurophysiol.* **79**, 1918–1930 (1998).
39. Ibbotson, M.R., Price, N.S., Crowder, N.A., Ono, S. & Mustari, M.J. Enhanced motion sensitivity follows saccadic suppression in the superior temporal sulcus of the macaque cortex. *Cereb. Cortex* **17**, 1129–1138 (2007).
40. Schmidt, M., Lehnert, G., Baker, R.G. & Hoffmann, K.P. Dendritic morphology of projection neurons in the cat pretectum. *J. Comp. Neurol.* **369**, 520–532 (1996).
41. Mustari, M.J., Fuchs, A.F. & Pong, M. Response properties of pretectal omnidirectional pause neurons in the behaving primate. *J. Neurophysiol.* **77**, 116–125 (1997).
42. Fischer, W.H., Schmidt, M. & Hoffmann, K.P. Saccade-induced activity of dorsal lateral geniculate nucleus X- and Y-cells during pharmacological inactivation of the cat pretectum. *Vis. Neurosci.* **15**, 197–210 (1998).
43. Cao, P., Gu, Y. & Wang, S.R. Visual neurons in the pigeon brain encode the acceleration of stimulus motion. *J. Neurosci.* **24**, 7690–7698 (2004).
44. Wang, S.R. & Matsumoto, N. Postsynaptic potentials and morphology of tectal cells responding to electrical stimulation of the bullfrog nucleus isthmi. *Vis. Neurosci.* **5**, 479–488 (1990).
45. Karten, H.J. & Hodos, W. *A Stereotaxic Atlas of the Brain of the Pigeon (Columba livia)* (The Johns Hopkins Press, Baltimore, Maryland, 1967).